Uncertainty Propagation for Classical Multi-dimensional Scaling Relative Localization

Derek Knowles
Mechanical Engineering
Stanford University
dcknowles@stanford.edu
December 2021

***Abstract*—Autonomous robots can often safely navigate in open-sky, outdoor environments by relying on global navigation satellite systems, like GPS, for accurate positioning estimates. However, the unavailability of satellite signals in certain locations, such as near tall buildings, trees, or other tall structures, can cause large uncertainty in the position estimates of autonomous robots. An alternative method to provide position estimation for a multi-robot system is to have nearby autonomous robots provide inter-ranging measurements with each other and use those measurements to perform relative localization. The proposed project looks at how to model position uncertainty of agents that are performing classical multi-dimensional scaling (MDS) relative localization using imperfect ranging measurements.**

***Index Terms*—multi-robot, uncertainty propagation, Euclidean Distance Matrix**

I. Introduction

Autonomous robots are being deployed around the globe in safety critical applications. In order to navigate in environments without colliding with buildings or other robots, each autonomous robot must be able to produce an accurate estimation of their position in the environment. Often autonomous robots make use of GNSS, global navigation satellite systems, signals to be able to produce position estimates. In outdoor, open-sky environments autonomous robots can receive GNSS signals from satellites across the sky which allows the robots to estimate their position with low uncertainty. However, buildings, trees, or other tall structures can block GNSS signals from reaching autonomous robots. When autonomous robots only receive a few number of GNSS signals, their position uncertainty rises.

An alternative method to providing position estimation is having a multi-robot system share inter-agent ranging measurements between neighboring robots.

In order to provide safety guarantees for robots moving around in an environment, it is desirable to be able to provide confidence bounds or a maximum error bound for their position solution. While confidence bounds for positioning using GNSS has been widely studied in the literature, it is unclear how to provide position estimate confidence bounds when localizing using inter-ranging measurements. Specifically, this project investigates understanding the *position* uncertainty of robots that are using inherently-uncertain inter-ranging measurements in order to localize themselves using an algorithm called classical Multi-dimensional scaling [1].

II. Related Work

Current work from the Stanford NAV Lab has developed Ultra-wide band (UWB) ranging radios that can be used by a multi-robot system to quickly exchange inter-ranging distances among each other [2]. An example multi-robot network is illustrated in Figure 1. However, these inter-ranging distances inherently have biases caused by inaccuracy in estimating the signal time of arrival and biases causes by the effects of signal reflection.

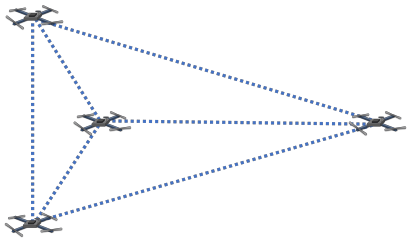

Fig. 1. Illustration of multi-robot network that is sharing inter-ranging measurements between all robots in the network.

Using techniques such as classical Multi-dimensional scaling [1], we can quickly use the noisy ranging measurements to estimate the relative distances between all pairs of robots in the network [3]. However, it is unclear how the errors in the measurements affect the position errors in the final localization result.

Algorithm 1: The classical MDS.

1: function `ClassicalMDS` (D, d)
2: $\quad J \leftarrow I - (1/n)\mathbf{1}\mathbf{1}^\top$ ▷ Geometric centering matrix
3: $\quad G \leftarrow -(1/2)\,JDJ$ ▷ Compute the Gram matrix
4: $\quad U, [\lambda_i]_{i=1}^n \leftarrow \mathrm{EVD}(G)$
5: $\quad$ return $[\mathrm{diag}(\sqrt{\lambda_1}, \ldots, \sqrt{\lambda_d}), 0_{d\times(n-d)}]\,U^\top$
6: end function

Fig. 2. Classical Multi-dimensional scaling (MDS) taken from [1] where D is a Euclidean distance matrix, d is the dimension of the state space, and EVD corresponds to the operation of eigenvalue decomposition.

One prior work has computed lower and upper intervals for the Euclidean distance matrix (defined in section III-B) which

is used in classical MDS [4]. The authors, however, make no attempt at describing the distribution of uncertainty itself.

In an alternative to the classical MDS algorithm, relative localization is also commonly performed using either linear or weighted least squares [5].

In terms of looking at the position uncertainty from simply using ranging measurements, one approach that already exists in this field is to use the directions of each measurement and the measurement variance to construct the Fisher information matrix for each agent [6]. The trace of the inverse of this matrix is called the Cramer-Rao bound and is a lower bound for the variance of an unbiased estimator. The Cramer-Rao lower bound utilizes the line-of-sight vectors between each robot and the sensor uncertainty in computing the bound. This bound is helpful for determining the best-case scenario of measurement error, but from a safety standpoint, what we're actually interested in is the worst-case scenario. Additionally, the Cramer-Rao bound does not tell us bounds for the mean of the error.

The goal of this project is to describe the position uncertainty distribution when using classical MDS for relative localization and compare the method to the optimal Cramer-Rao lower bound for the robot configuration.

III. Approach

Consider a system with n robots that is fully-connected (i.e. all robots can communicate with all other robots). The measured range of robot A to robot B is written as $\tilde{r}_{AB}$ and that measured range is assumed to be identical between the two robots, $\tilde{r}_{AB} = \tilde{r}_{BA}$. Robot A measuring the range to robot B, $\tilde{r}_{AB}$, will obtain the same measurement as robot B measuring the range to robot A, $\tilde{r}_{BA}$.

We will now progress through each step of the classical MDS algorithm shown in Figure 2 in order to determine the final position uncertainty of classical MDS. For this example, we will use a robot configuration similar to Figure 1.

A. Initial Measurement Distribution

The measured range between each robot is assumed to be a function of the true range between each robot and normally distributed sensor noise according to the following equation:

$$\tilde{r} = r + \xi \tag{1}$$

where $\xi \sim \mathcal{N}(0, \sigma^2_{UWB})$. Thus the measured range can actually be written as a Gaussian distribution with a nonzero mean, $\tilde{r} \sim \mathcal{N}(r, \sigma^2_{UWB})$. The result is shown in Figure 3 for 10,000 random measurement samples along with the expected Normal distribution for each measurement.

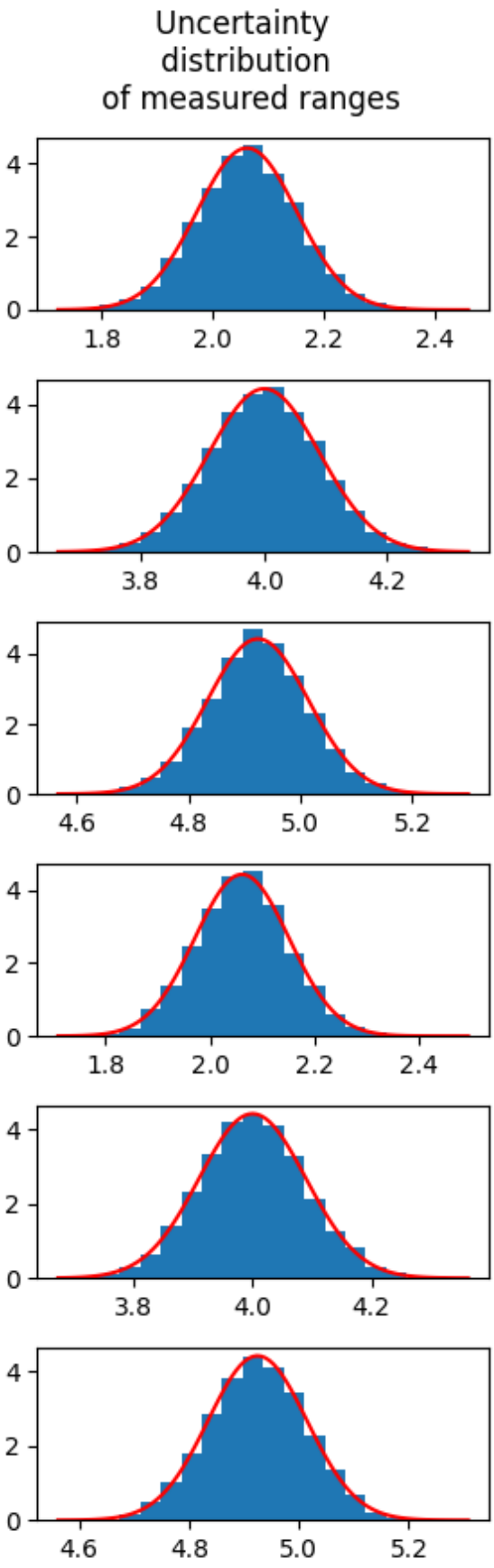

Fig. 3. Distribution of initial measured ranges with the expected Normal distribution outlined in red.

B. Squared Measurement Distribution

If a random variable is sampled from a Normal distribution (i.e., $X \sim \mathcal{N}(\mu, \sigma^2)$), then the distribution for its square is a noncentral Chi-squared distribution with a single degree of freedom, a noncentrality parameter of $\left(\frac{\mu}{\sigma}\right)^2$, and scaled by σ^2 [7].

This result is shown in Figure 4 for 10,000 random measurement samples along with the expected noncentral, scaled Chi-squared distribution for each measurement.

This means that the distribution for the squared ranges, $\tilde{r}^2$, will have the form of

$$X^2 \sim \sigma_{UWB}^2 \left(\chi^2 \left(k = 1, \lambda = \left(\frac{r}{\sigma_{UWB}} \right)^2 \right) \right) \tag{2}$$

The corresponding Euclidean distance matrix, D, is comprised of the squared ranges between all pairs of robots in the system. The Euclidean distance matrix can then be constructed and written as:

$$D = \begin{bmatrix} 0 & \tilde{r}_{12}^2 & r_{13}^2 & \cdots & \tilde{r}_{1n}^2 \\ \tilde{r}_{21}^2 & 0 & r_{23}^2 & \cdots & \tilde{r}_{2n}^2 \\ \tilde{r}_{31}^2 & r_{32}^2 & 0 & \cdots & \tilde{r}_{3n}^2 \\ \vdots & \vdots & \vdots & \ddots & \vdots \\ \tilde{r}_{n1}^2 & r_{n2}^2 & r_{n3}^2 & \cdots & 0 \end{bmatrix} \tag{3}$$

C. Gram Matrix from Double Centering

We have now computed the uncertainty distribution for the Euclidean distance matrix input D in the classical MDS algorithm shown in 2. We now will derive the uncertainty distribution of the elements in the Gram matrix, G. The Gram matrix, G, is obtained from the Euclidean distance matrix, D, in a process called double centering [8]. In classical MDS, this step is performed as

$$G \leftarrow -\left(\frac{1}{2}\right) JDJ \tag{4}$$

This means that the elements of the Gram matrix are all linear combinations of the scaled noncentral Chi-squared distributions with degree of freedom n. As an example, in the case where we have four robots all exchanging ranges with each other, i.e., $n = 4$, then the top left element of the Gram matrix, G_{11}, is a weighted combination of ten separate elements of the Euclidean Distance matrix according to the following formula:

$$\begin{aligned} G_{11} = {} & 0.09375D_{12} + 0.03125D_{13} + 0.09375D14 \\ & + 0.09375D_{21} - 0.03125D_{24} + 0.09375D_{31} \\ & + 0.03125D_{32} - 0.03125D_{34} \\ & + 0.09375D_{41} - 0.03125D_{42} \end{aligned} \tag{5}$$

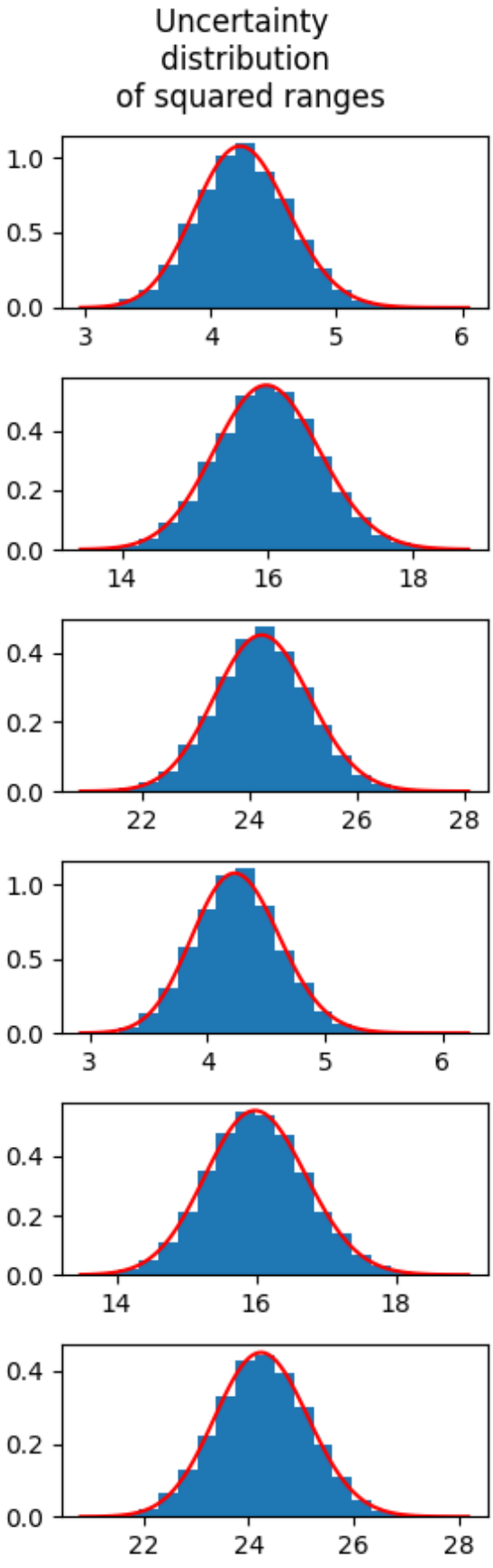

Fig. 4. Distribution of squared measured ranges with expected noncentral, scaled Chi-squared distribution for each measurement shown in red.

D. Eigenvalue Decomposition and Position Uncertainty

The final two steps of eigenvalue and decomposition essentially retrieve the symmetric part of the lower component part of the Gram matrix. The part where you only use up to d eigenvalues in line 5 of the MDS algorithm shown in Figure 2 means that you are essentially doing principal component analysis and retrieving the d (the dimension of the state space) number of elements.

IV. Results

To enable rapid testing of the MDS algorithm, I created a vectorized version of the algorithm through numpy and pytorch operations. This method allowed me to create an interactive visualization that is responsive despite doing 10,000 iterations. The interface for the interactive visualization is shown in Figure 8.

Figure 5 shows that when positions are sort of uniformly distributed, the final position distributions shown in Figure 6 look somewhat Gaussian. However, when the geometry of the robots move into other shapes like Figure 7 the final position uncertainty is clearly multi-modal and no longer gaussian.

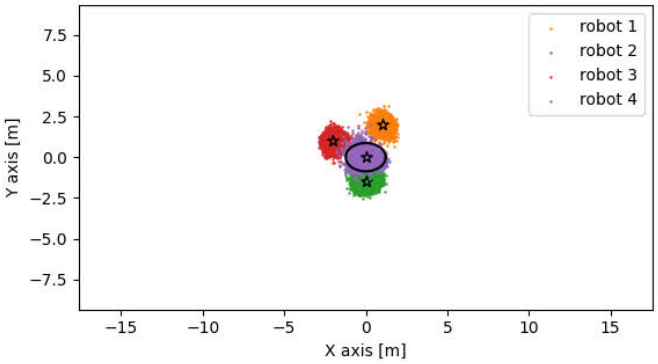

Fig. 5. Map of final position uncertainty distributions in a simple scenario with the Cramer-Rao lower bound for the fourth robot plotted in black.

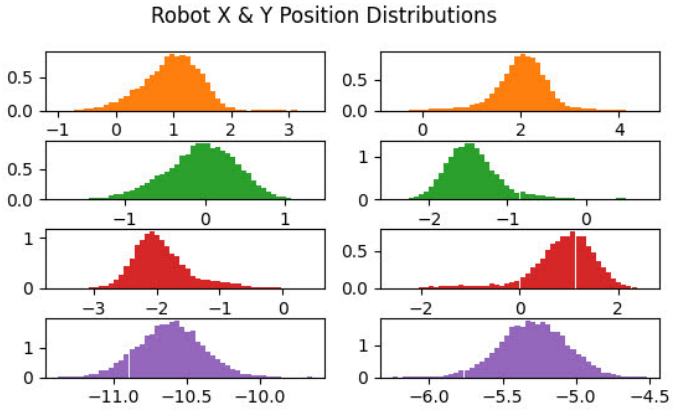

Fig. 6. Final X Y position distributions corresponding to the robot configuration in Figure 5.

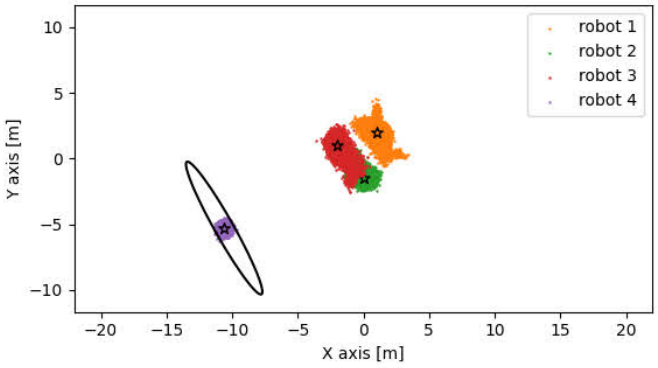

Fig. 7. Map of final position uncertainty distributions with the Cramer-Rao lower bound for the fourth robot plotted in black.

Additionally, the dark ellipse in Figures 5, 7, 9, and 10 shows the computed Cramer-Rao lower bound for the specific geometry. The Cramer-Rao lower bound is computed as the inverse of the Fisher information matrix. The Fisher information matrix computation was simplified for ranging measurements in [9] as:

$$FI = \frac{1}{\sigma_{UWB}} \sum_{i=1}^{n} \begin{bmatrix} \sin^2(\phi_i) & \frac{\sin(2\phi_i)}{2} \\ \frac{\sin(2\phi_i)}{2} & \cos^2(\phi_i) \end{bmatrix}, \tag{6}$$

which shows that the Fisher information matrix, FI, is computed using the standard deviation of the measurements, σ_{UWB}, and a sum of matrices based on the line-of-sight direction between the two agents for all n number of neighbors. The Fisher information matrix must be computed for each robot individually. In our results, we only compute the matrix for robot 4, although the math will be extended in the future for all robots. The Cramer-Rao lower bound is the inverse of the Fisher information matrix and represents the lower bound of the covariance that can be achieved by an unbiased estimator [9].

Interestingly, Figure 9 shows that the shape of the Cramer-Rao lower bound is different than the shape of the EDM position distribution. If you notice, the skew of the ellipse for the EDM distribution is actually opposite from what the Cramer-Rao lower bound predicts. This may simply be from the fact that the EDM formulation is not an unbiased estimator (an assumption for the Fisher Information matrix). Looking into being able to provide a tighter bound will be investigated in future work.

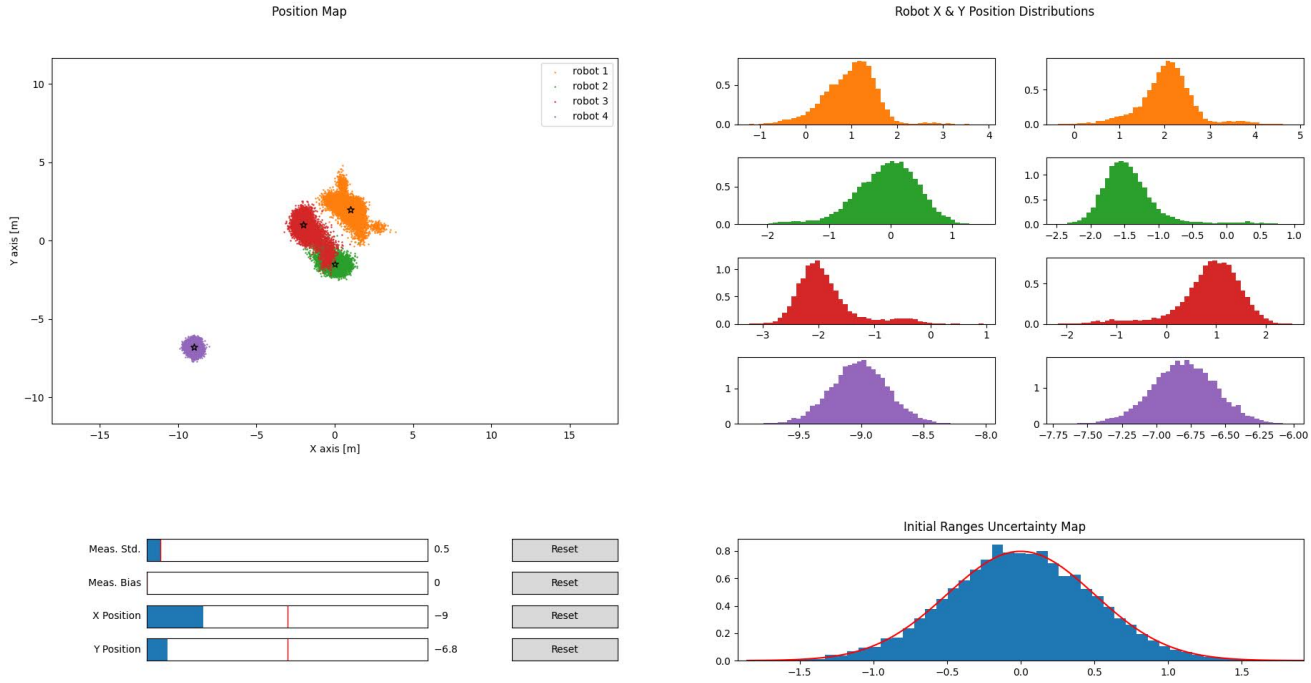

Fig. 8. Interactive EDM Visualization.

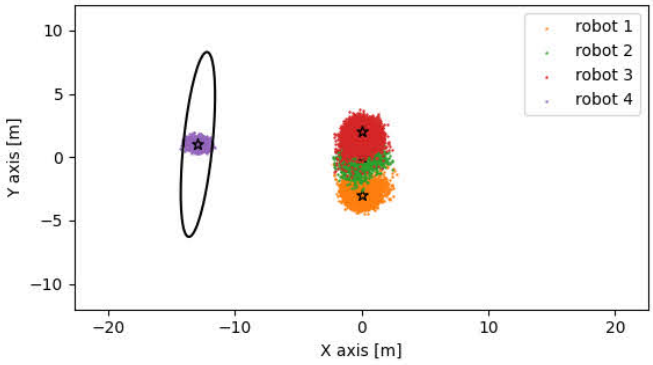

Fig. 9. Map of final position uncertainty distributions with the Cramer-Rao lower bound for the fourth robot plotted in black.

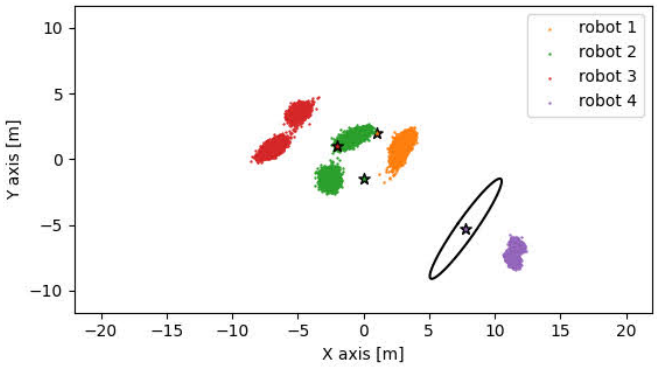

Fig. 10. Map of final position uncertainty distributions for a scenario with large added bias with the Cramer-Rao lower bound for the fourth robot plotted in black.

Figure 10 demonstrates a scenario with added bias to the measurements and how added bias can create disjoint bi-modal position uncertainties shown if Figure 11. This modal result is extremely undesirable and so thanks to this research, more effort will be put into eliminating biases from our lab's ranging sensors.

V. Conclusions

This project has shown the position distribution of relative localization using ranging measurements. I compared the position uncertainties obtained from classical MDS with the Cramer-Rao optimal lower bound for each provided configuration.

Although this work used many heavy assumptions (e.g., Gaussian, zero-mean distribution for sensor noise), the project provided useful insight into the position uncertainty distribution and allow for safer robot algorithms in the future.

References

[1] I. Dokmanic, R. Parhizkar, J. Ranieri, and M. Vetterli, "Euclidean Distance Matrices: Essential theory, algorithms, and applications," *IEEE Signal Processing Magazine*, vol. 32, no. 6, pp. 12–30, nov 2015.

[2] D. Stier, A. Wu, A. Mohanty, and G. Gao, "A test platform for uwb-based localization of dynamic multi-agent systems," in *ICRA*, 2022.

[3] S. Albanie, "Euclidean Distance Matrix Trick," jun 2019. [Online]. Available: https://www.robots.ox.ac.uk/∼albanie/notes/Euclidean_distance_trick.pdf

[4] H. S. Ahn and K. K. Oh, "Command coordination in multi-agent formation: euclidean distance matrix approaches," in *ICCAS 2010 - International Conference on Control, Automation and Systems*, 2010, pp. 1592–1597.

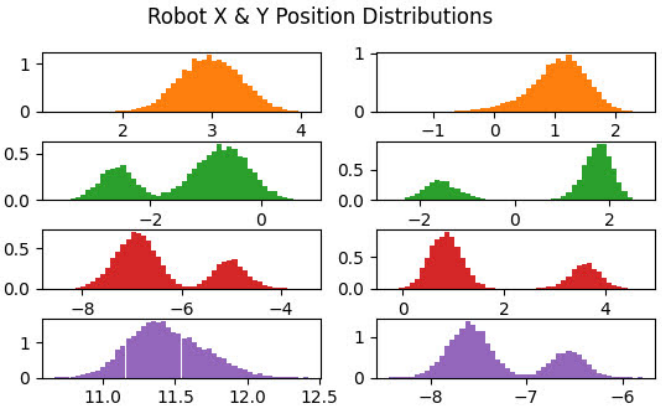

Fig. 11. Final X Y position distributions corresponding to the robot configuration in Figure 10.

[5] Y. Wang, "Linear least squares localization in sensor networks," *Eurasip Journal on Wireless Communications and Networking*, vol. 2015, no. 1, pp. 1–7, mar 2015. [Online]. Available: https://jwcn-eurasipjournals.springeropen.com/articles/10.1186/s13638-015-0298-1

[6] S. Zhang, R. Pöhlmann, T. Wiedemann, A. Dammann, H. Wymeersch, and P. A. Hoeher, "Self-aware swarm navigation in autonomous exploration missions," *Proceedings of the IEEE*, vol. 108, no. 7, pp. 1168–1195, 2020.

[7] J. (https://stats.stackexchange.com/users/31420/johnk), "Pdf of the square of a standard normal random variable," Cross Validated, uRL:https://stats.stackexchange.com/q/192822 (version: 2019-05-05). [Online]. Available: https://stats.stackexchange.com/q/192822

[8] J. Dattorro, *Convex Optimization: Euclidean Distance Geometry*. Palo Alto: Meboo, 2015.

[9] A. N. Bishop, B. Fidan, B. D. Anderson, K. Doğançay, and P. N. Pathirana, "Optimality analysis of sensor-target localization geometries," *Automatica*, vol. 46, no. 3, pp. 479–492, mar 2010.